

# Collision Detection Algorithm of Belt Grinding of the Blisk Based on Improved Octree Segmentation Method

Zhi Huang (✉ [zhihuang@uestc.edu.cn](mailto:zhihuang@uestc.edu.cn))

School of Mechanical and Electrical Engineering, University of Electronic Science and Technology of China, Chengdu, China

Xing Yang

University of Electronic Science and Technology of China

Jie Min

School of Mechanical and Electrical Engineering, University of Electronic Science and Technology of China, Chengdu, China

Hongyan Wang

School of Mechanical and Electrical Engineering, University of Electronic Science and Technology of China, Chengdu, China

Pengxuan Wei

School of Mechanical and Electrical Engineering, University of Electronic Science and Technology of China, Chengdu, China

---

## Research Article

**Keywords:** Belt grinding, collision detection, bounding box, k-means clustering algorithm, improved octree segmentation method

**Posted Date:** June 14th, 2021

**DOI:** <https://doi.org/10.21203/rs.3.rs-582123/v1>

**License:**  This work is licensed under a Creative Commons Attribution 4.0 International License.

[Read Full License](#)

---

# **Collision detection algorithm of belt grinding of the Blisk based on improved octree segmentation method**

**Zhi Huang<sup>1</sup>, Xing Yang<sup>1</sup>, Jie Min<sup>1</sup>, Hongyan Wang<sup>1</sup> and Pengxuan Wei<sup>1</sup>**

<sup>1</sup>School of Mechanical and Electrical Engineering, University of Electronic Science and Technology of China, Chengdu, China

## **Corresponding author:**

Zhi Huang, University of Electronic Science and Technology of China, Chengdu 611731, China.

Email: zhihuang@uestc.edu.cn

## **Abstract**

In the process of belt grinding aero-engine Blisk(Bladed Disk), the abrasive belt can easily interfere with the Blisk, which will damage the valuable Blisk. Therefore, it is indispensable and significant to study the collision detection of belt grinding the Blisk. However, the application of traditional collision detection algorithms in this complicated realistic scene is difficult to obtain satisfactory results. In order to improve the accuracy and efficiency of the collision detection of grinding the Blisk, a collision detection algorithm based on the improved octree segmentation method is proposed in this paper. Firstly, the Oriented Bounding Box (OBB) is applied to establish the collision detection model for the abrasive belt. Secondly, the traditional octree segmentation method is optimized based on the k-means clustering algorithm, and an improved octree segmentation method is presented, in addition, the flow chart of the collision detection algorithm for belt grinding of the Blisks given. Finally, algorithm verification and experimental verification are carried out based on a certain type of the Blisk. The results suggest that compared with the traditional method, the method in this paper not only promotes the accuracy of collision detection, but also promotes the efficiency of collision detection, and meets the requirements of object collision detection in this tanglesome scene with both accuracy and speed.

## **Keywords**

Belt grinding, collision detection, bounding box, k-means clustering algorithm, improved octree segmentation method

## **Declarations**

**Funding:** The Fundamental Research Funded by Sichuan Science and Technology Plan (grant number: 2020YFG0407/2020JDRC0173).

**Conflicts of interest/Competing interests:** We have no potential conflict of interest to declare.

**Availability of data and material:** All data generated or analysed during this study are included in this manuscript.

**Code availability:** Our research is supported by code. If you want to get the code, please contact the corresponding author of this paper.

**Ethics approval:** Not applicable.

**Consent to participate:** Yes, we agreed to participate.

**Consent for publication:** Not applicable.

## 1 Introduction

The Blisk plays a decisive role in the manufacture and production of aero engines [1]. Blisks are one of the key parts of aero engine, its profile is thin and twisted, and its flow channel is deep and narrow, making it difficult to machine. Therefore, its precision machining has become the key in the field of aero engine manufacturing. Belt grinding is one of the commonly used methods for the precision machining of the Blisk of the engine [2]. When the belt grinding is processed, the belt and the Blisk are easily interfered, which will damage the valuable Blisk. Therefore, it is very crucial to study the collision detection of the Blisk grinding with abrasive belt [3, 4, 5].

Collision detection plays a very important role in many fields, such as computer simulation, robot motion path planning, and machine tool processing simulation, etc [6]. Collision detection requires accurate collision location information, but the speed and accuracy of detection are contradictory. In order to solve this problem, many experts and scholars have conducted a lot of research on the efficiency and accuracy of collision detection in recent years. In order to solve the collision interference problem in robot belt grinding, Zhang et al. [7] proposed a collision-free planning algorithm for robot motion paths based on the collision layer method. The algorithm uses neighborhood search and recursive methods to quickly find the planning curve in the collision layer, thereby significantly reducing the number of collision detections. Ren et al. [8] proposed an enhanced geometric representation technology based on the surface approximation points, which simplifies the simulation of robot belt grinding through the DOP-tree positioning algorithm, and improves the speed of collision detection. For the purpose of improving the efficiency of collision detection, TANG et al. [9] proposed a collision detection algorithm based on the combination of mass point conversion and bounding box, which constructs

the OBB hierarchical bounding box by using the area center method and binary tree for all objects in the space. Prasanth et al. [10] studied the collision detection strategy of sheet metal bending problems, and concluded that the collision detection method based on AABB(Axis-aligned bounding box) can be better integrated with sheet metal bending planning, and further realized the integration of computer-aided design and computer-aided manufacturing. In order to ensure high accuracy and meet real-time requirements, Zou et al. [11] proposed a fast software collision detection algorithm, which is a combination of random method and adaptive Cauchy mutation particle swarm algorithm. Sang et al. [12] studied the collision relationship between the five-axis CNC machine tool and the workpiece, and optimized the collision detection algorithm of the traditional CNC machine tool by using the collision detection algorithm of the rectangular parallelepiped and the separated axis, which improved the detection efficiency and accuracy. Tang et al. [13] proposed a collision algorithm based on the maximum collision box to automatically detect and correct collisions. The author finally integrated the algorithm into the software and successfully applied it to the collision detection of five-axis CNC machining. The above research results have improved the efficiency and accuracy of object collision detection to a certain extent, but how to improve the accuracy and efficiency of collision detection between complex models in complex realistic scenes is still a formidable challenge. The collision detection of the Blisk of abrasive belt grinding belongs to the collision detection problem between complex models in complex realistic scenes. In order to improve the accuracy and efficiency of collision detection in this environment, this paper proposes a collision detection algorithm for the Blisk of belt grinding based on the improved octree segmentation method. The main work of this paper is as follows: Firstly, the OBB is applied to establish the

collision detection model of the abrasive belt; secondly, the traditional octree segmentation method is optimized based on the k-means clustering algorithm. The proposed method can better reduce the detection range and generate the number of bounding boxes in the accurate detection stage, thereby improving the accuracy of collision detection and reducing the time required for collision detection; finally, experimental verification is taken to confirm our method for abrasive belt grinding a certain type of the Blisk.

## 2 Basic collision detection algorithm model

### 2.1 The principle of belt grinding the Blisk

At present, the aero-engine Blisk is mainly used for precision milling to ensure their profile accuracy. However, due to the weak structural rigidity and complex profiles of the blade of the Blisk, it is difficult to ensure the profile and shape of the blade after milling. Therefore, the blade must be ground with abrasive belt after precision milling to ensure its profile shape and profile quality [14]. The principle diagram of belt grinding the Blisk is shown in Figure 1. Abrasive belt grinding is a composite processing method, it tensions the abrasive belt by means of a tensioning mechanism, drives the abrasive belt to move at a high speed under the action of the driving wheel, and under a certain pressure, makes the abrasive belt come into contact with the surface of the workpiece to realize the entire grinding process.

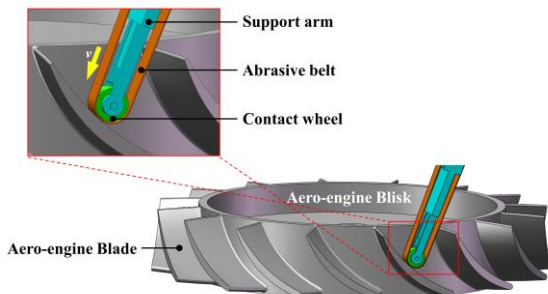


**Fig. 1** The principle diagram of belt grinding the Blisk

### 2.2 OBB bounding box model of abrasive belt

Bounding box is an algorithm for solving the optimal enclosing space of a set of discrete points. Its basic idea is to use simple geometric bodies (called bounding box) to approximately replace complex geometric objects, so as to achieve the purpose of rapid collision detection [15]. OBB is defined as the smallest regular hexahedron that contains the object and is arbitrarily oriented relative to the coordinate axis. Its biggest feature is that the direction of the bounding box is arbitrary, which makes it possible to tightly surround the object. The key point of establishing the OBB bounding box model is to find the best direction of the smallest regular hexahedron and determine the minimum size of the bounding box in this direction.

First of all, according to the above theory, the process of establishing the bounding box model of abrasive belt OBB in this paper is as follows:

Step1. Use the PCA principal component analysis method to obtain the three principal directions ( $x$ -axis,  $y$ -axis and  $z$ -axis), centroid and covariance matrix of the abrasive belt point cloud, and obtain its eigenvalue and eigenvector by solving the matrix. The eigenvector is the main direction;

Step2. Use the main direction and center of mass obtained in Step1 to convert the input point cloud to the origin, and the main direction coincides with the coordinate system direction, and establish a point cloud bounding box transformed to the origin;

Step3. Obtain the main direction and bounding box of the input point cloud through the inverse transformation of the input point cloud to the origin point cloud.

Secondly, let any point in the abrasive belt point cloud be  $P_i = (x_i, y_i, z_i)$  ( $1 \leq i \leq 19499$ ) (because the number of abrasive belt point clouds used in this paper is 19499, the value of  $i$  is  $1 \sim 19499$ ),  $\text{PointsSet}$  represents the point cloud collection, and  $C$  represents the association, then

$$\text{PointsSet} = \begin{bmatrix} \mathbf{P}_1 \\ \mathbf{P}_2 \\ \mathbf{K} \\ \mathbf{P}_n \end{bmatrix} = \begin{bmatrix} (x_1, y_1, z_1) \\ (x_2, y_2, z_2) \\ \vdots \\ (x_n, y_n, z_n) \end{bmatrix} = [X \ Y \ Z] \quad (1)$$

$$C = \begin{bmatrix} \text{cov}(X, X) & \text{cov}(X, Y) & \text{cov}(X, Z) \\ \text{cov}(Y, X) & \text{cov}(Y, Y) & \text{cov}(Y, Z) \\ \text{cov}(Z, X) & \text{cov}(Z, Y) & \text{cov}(Z, Z) \end{bmatrix} \quad (2)$$

where,

$$\left\{ \begin{array}{l} \bar{X} = \frac{\sum_{i=1}^n X_i}{n}, \bar{Y} = \frac{\sum_{i=1}^n Y_i}{n}, \bar{Z} = \frac{\sum_{i=1}^n Z_i}{n} \\ \text{cov}(X, Y) = \frac{\sum_{i=1}^n (X_i - \bar{X})(Y_i - \bar{Y})}{n-1}, \\ \text{cov}(Y, Z) = \frac{\sum_{i=1}^n (Y_i - \bar{Y})(Z_i - \bar{Z})}{n-1}, \\ \text{cov}(Z, X) = \frac{\sum_{i=1}^n (Z_i - \bar{Z})(X_i - \bar{X})}{n-1}. \end{array} \right. \quad (3)$$

Finally, the OBB bounding box model of the abrasive belt is established, as shown in Figure 2.

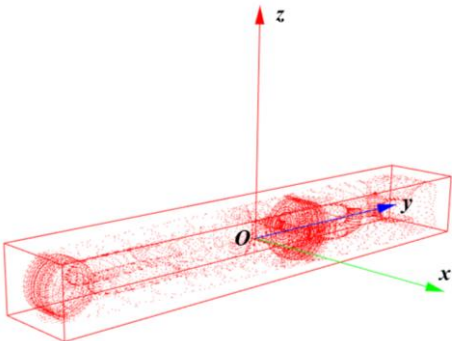


**Fig. 2** OBB bounding box model of the abrasive belt

### 2.3 Octree segmentation method of the Blisk

The octree is a recursive, axis-aligned and space-separated data structure. It divides limited three-dimensional data into 8 nodes. Dividing the space into cubes of equal size can speed up calculations and save storage space. The principle diagram of the octree segmentation method is shown in Figure 3.

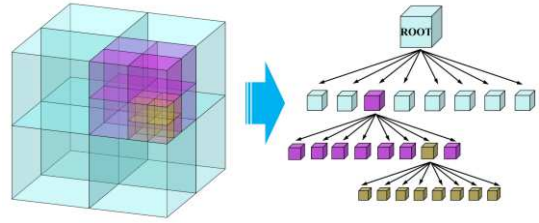


**Fig. 3** Schematic diagram of octree segmentation method

Since the blade of the Bliskis complex free-form surface, the tool points in the machining path planning are uneven. In order to facilitate the collision detection process, this paper adopts an octree segmentation method with a fixed number of points (that is, each tree node that meets the condition contains a fixed number of points, which is the basis for the termination of the octree split in this paper) to segment its space. The use of this processing method is conducive to the division of the processing space, which can improve the collision detection efficiency between the abrasive belt and the Blisk to a certain extent.

## 3 Improved collision detection algorithm model

### 3.1 Limitations of traditional octree segmentation method

For convenience, we first study the individual blade of the Blisk, and then apply the results of the research to the Blisk. Figure 4 shows the traditional segmentation results of a single blade of the Blisk under different fixed points (that is, each tree node that meets the condition contains a fixed number of points).

It can be seen from Figure 4 that as the number of fixed points gradually increases, the segmentation accuracy of the octree will gradually decrease. Therefore, in order to ensure the accuracy of the collision detection of the Blisk for belt grinding, in the follow-up research of this paper, the number of fixed points selected does not exceed 10.

The above-mentioned traditional octree fixed-point division processing method can accelerate

the division of the processing space to a certain extent, and improve the collision detection efficiency between the abrasive belt and the Blisk. However, as can be seen from Figure 4, this segmentation processing method cannot effectively eliminate the redundant space, thereby

greatly reducing the accuracy of collision detection. In addition, when high-precision collision detection is required, the traditional method generates a large number of redundant enclosures, which further greatly reduces the efficiency of collision detection.

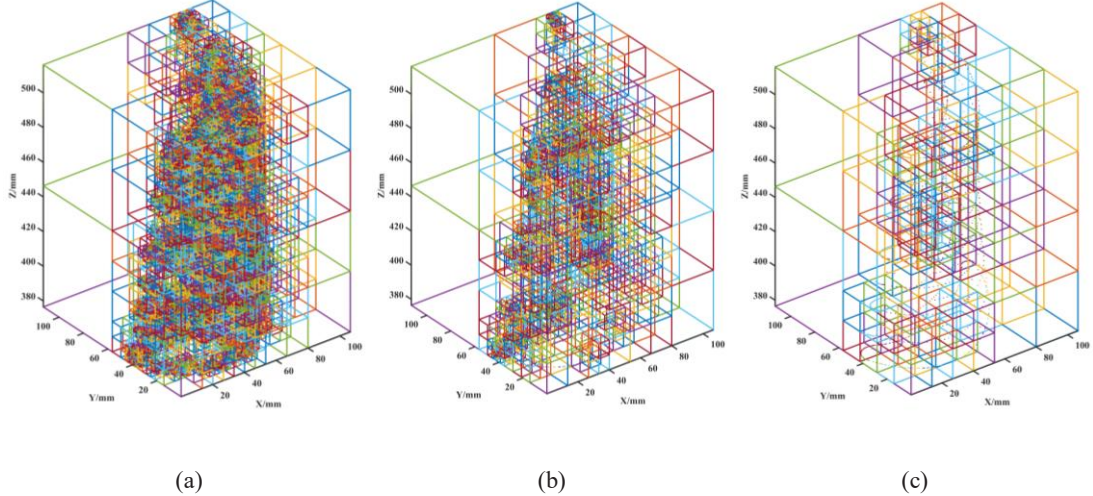


**Fig. 4** Octree segmentation results of the blade under different fixed points((a) the number of fixed points is 2, (b) the number of fixed points is 10, (c) the number of fixed points is 50)

### 3.2 Improved octree segmentation method based on k-means clustering algorithm

In order to solve the many shortcomings caused by the above-mentioned traditional methods, this paper adopts the idea of "divide and conquer, overall optimization", and introduces the k-means clustering algorithm [16] to improve it, that is, firstly, perform appropriate point cloud classification of the individual blades of the Blisk, then perform the octree segmentation after classification respectively, finally, the result is stored in the corresponding data structure for subsequent collision detection.

In this paper, the Euclidean distance between data objects [17] is used as the basis of *k-means* algorithm clustering, where  $k$  represents the number of clusters, and *means* represents the mean value of the data objects in the clusters. It should be pointed out that the change of  $k$  value will affect the result of clustering. In order to find the best  $k$  value of *k-means* clustering algorithm, the range of  $k$  value is 2~8 in this paper.

For a given data set  $D = \{d_1, d_2, d_3, \dots, d_n\}$  containing  $n$  dim-dimensional data points, where  $d_i \in R^{\text{dim}}$ . Now we have to use the *k-means* clustering algorithm to divide the data set into  $k$  clusters, and we use  $C$  to represent the set of  $k$  clusters, that is:  $C = \{C_1, C_2, \dots, C_k\}$ . For each divided cluster  $C_j (j = 1, 2, \dots, k)$ , there must be a center point  $\mu_j (j = 1, 2, \dots, k)$  in it. Generally, the Euclidean distance is selected as the criterion for judging the similarity and distance of each data in the cluster. Assuming that the sum of the squares of the distances from each point in the cluster to its center point  $\mu_j (j = 1, 2, \dots, k)$  is  $S(C_j) (j = 1, 2, \dots, k)$ , then

$$S(C_j) = \sum_{d_i \in C_j} \|d_i - \mu_j\|^2 \quad (i = 1, 2, \dots, n; j = 1, 2, \dots, k) \quad (4)$$

Obviously, the purpose of using the clustering algorithm is to minimize the formula (5).

$$\begin{aligned}
S(C) &= \sum_{j=1}^k S(C_j) \\
&= \sum_{j=1}^k \sum_{d_i \in C_j} \|d_i - \mu_j\|^2 \quad (i = 1, L, n; j = 1, L, k)
\end{aligned} \tag{5}$$

The steps for applying the algorithm in this paper are as follows:

Step 1. Enter the number of clusters  $k$  and the data set  $D = \{d_1, d_2, d_3, L, d_n\}$  containing  $n$  dim (in this paper, dim=3) dimensional data points, where  $d_i \in R^{\text{dim}}$ , and randomly select  $k$  initial center points  $\mu_1, L, \mu_k$ ;

Step 2. Calculate the distances from all data points  $d_i (i = 1, 2, L, n)$  in the data set to these  $k$  initial center points respectively. If any data point  $d_i (i = 1, 2, L, n)$  in the data set is closest to the initial center point  $\mu_j (j = 1, L, k)$ , then this data point  $d_i (i = 1, 2, L, n)$  will be divided into cluster  $C_j (j = 1, 2, L, k)$ ; if the distances to multiple initial center points are equal, they can be divided into arbitrary clusters. Any data point  $d_i (i = 1, 2, L, n)$  is divided into cluster  $C_j (j = 1, 2, L, k)$  to satisfy:

$$C_j = \{d_i : \|d_i - \mu_j\|^2 \leq \|d_i - \mu_{j'}\|^2, \forall j, \forall j', 1 \leq j \leq k, 1 \leq j' \leq k\}.$$

Step 3. After classifying all the data points, calculate the mean value in each cluster as the new center point of the cluster. This process is also called updating the cluster mean;

Step 4. Repeat steps 2 and 3 until the new center point of the cluster is equal to the initial center point, and output a data set of  $k$  clusters.

Step 5. Find the optimal  $k$  value of the data set analysis results in the  $k$  clusters in step 4, record it as  $k_{opt}$ , and output the data set of the  $k_{opt}$  cluster. At this time, the algorithm ends.

The improved octree segmentation method based on  $k$ -means clustering algorithm can effectively eliminate redundant space, make the divided area more reasonable, make the area involved in collision detection smaller, so that the accuracy and efficiency of collision detection can be achieved at the same time. The principle

diagram of the comparison of the partition space with the traditional octree partition method is shown in Figure 5.

It can be seen from Figure 5 that the improved octree segmentation method is more accurate in space segmentation than the traditional octree segmentation method. This obviously improves the accuracy of collision detection and improves the efficiency of collision detection due to less redundant space. Therefore, the new method will help improve the accuracy and efficiency of collision detection at the same time.

### 3.3 Collision detection algorithm

The definition of the separation axis theorem is as follows [18, 19]: if an axis can be found in the three-dimensional space of the target object, and the two target objects are projected on the axis separately, and no overlapping projection part can be found on the axis, then this axis is defined as the separation axis.

Suppose  $O_a$  and  $O_b$  are the hierarchical enclosing volume models of two target objects in space. In this paper, a straight line parallel to the  $X$  direction of the  $O_a$  enclosing volume is taken as the separation axis of the two.

In Figure 6,  $a_1, a_2, a_3$  and  $b_1, b_2, b_3$  are the half lengths of the orthogonal edges of the  $O_a$  and  $O_b$  enclosing bodies;  $V_a^1, V_a^2, V_a^3$  and  $V_b^1, V_b^2, V_b^3$  are the three-dimensional coordinate axis space vectors respectively;  $C_a$  and  $C_b$  are the center points respectively;  $\mathbf{n}$  is the separating axis vector (it is not necessarily a unit vector). In this paper, the vertices of  $O_a$  and  $O_b$  are projected on the separating axis  $\mathbf{n}$ , and the length of the vector formed by the projection line of  $C_a$  and  $C_b$  on the separating axis  $\mathbf{n}$  is  $L$ , which is:

$$L = \frac{C_a C_b \mathbf{n}}{|\mathbf{n}|} \tag{6}$$

where,

$$C_a C_b = \frac{|C_a \mathbf{n} - C_b \mathbf{n}|}{|\mathbf{n}|} = \frac{(C_a - C_b) \mathbf{n}}{|\mathbf{n}|}. \tag{7}$$

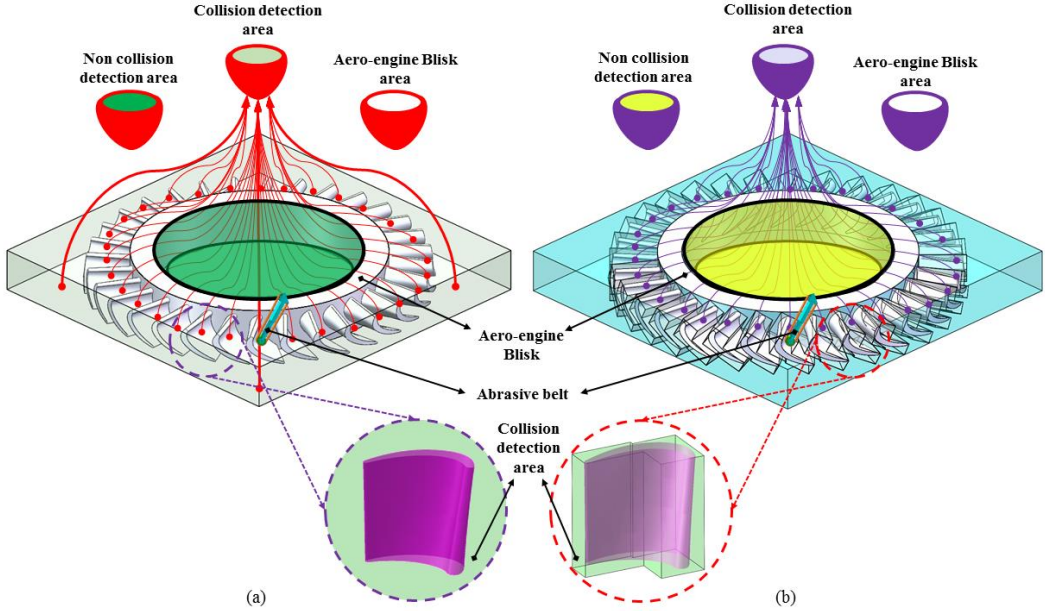


**Fig. 5** Comparison of spatial segmentation between traditional octree segmentation method and improved octree segmentation method ((a)traditional octree segmentation method, (b)improved octree segmentation method)

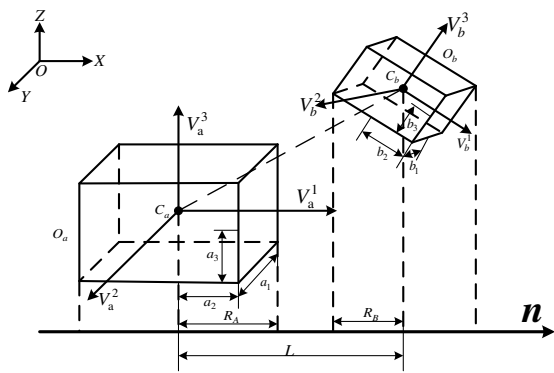


**Fig. 6** The principle diagram of the collision detection of the separation axis method [20]

According to Fig. 6, the side length projection and the center point projection of the two enclosing bodies on the separating axis can be obtained, thereby obtaining the half length of the orthogonal side projection and the length of the line connecting the two center point projections. If the length  $L$  of the connecting line between the center point projections  $C_a$  and  $C_b$  is greater than the sum of the corresponding half lengths of the orthogonal side projections, that is, if formula (8) is satisfied, it means that the two enclosing bodies do not intersect, otherwise, they intersect.

$$L > R_A + R_B \quad (8)$$

In the above formula,  $R_A$  and  $R_B$  are the length of the projection line of the center point and vertex of  $O_a$  and  $O_b$  respectively on the separating axis:

$$R_A = \frac{a_1 |V_a^1 \mathbf{n}| + a_2 |V_a^2 \mathbf{n}| + a_3 |V_a^3 \mathbf{n}|}{|\mathbf{n}|} \quad (9)$$

$$R_B = \frac{b_1 |V_b^1 \mathbf{n}| + b_2 |V_b^2 \mathbf{n}| + b_3 |V_b^3 \mathbf{n}|}{|\mathbf{n}|} \quad (10)$$

Combining equations (9) and (10) into equation (8), we can get:

$$\begin{aligned} & |(C_a - C_b) \mathbf{n}| > a_1 |V_a^1 \mathbf{n}| + a_2 |V_a^2 \mathbf{n}| + a_3 |V_a^3 \mathbf{n}| \\ & + b_1 |V_b^1 \mathbf{n}| + b_2 |V_b^2 \mathbf{n}| + b_3 |V_b^3 \mathbf{n}| \end{aligned} \quad (11)$$

Finally, the flow chart of the collision detection algorithm in this paper is shown in Figure 7.

## 4 Experimental results and analysis

### 4.1 Experimental results and analysis of improved octree segmentation method

Firstly, in order to find the best  $k$  value of the  $k$ -means clustering algorithm, experiments were carried out on a single blade of the Blisk, and the result shown in Fig. 8 was obtained.

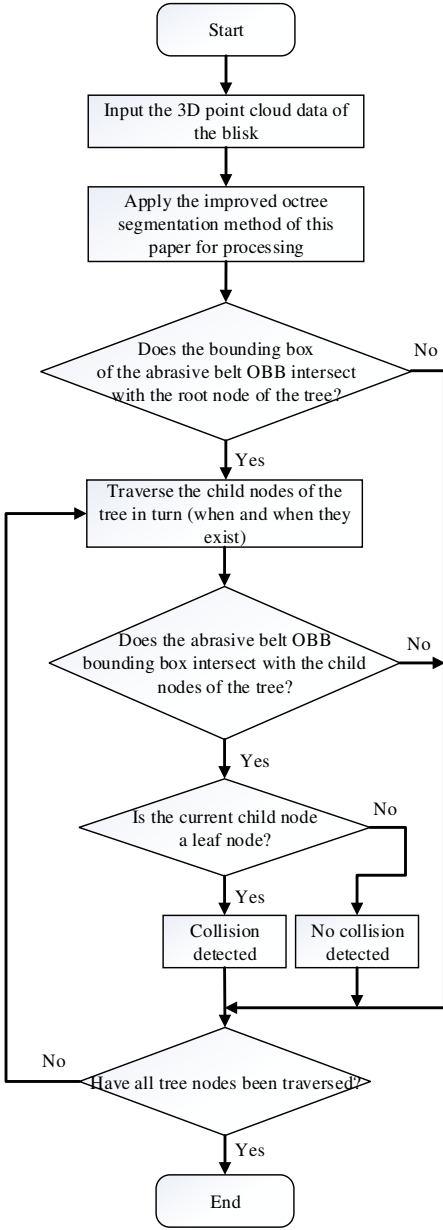


**Fig. 7** Flow chart of collision detection algorithm in this paper

Then, the improved octree segmentation method was used to experiment on a single blade of the Blisk. The experimental results are as follows. The comparison of the total number of split nodes between the traditional octree split method and the improved octree split method is shown in Table 1, and the split time comparison between the traditional octree split method and the improved octree split method is shown in Table 2. The comparison chart is shown in Figure 9 and Figure 10 respectively. It is worth pointing out that according to the clustering results

obtained in the above experiment, the mean value of all data points in each cluster is calculated, so as to ensure that the initial center point of the cluster in the collision detection algorithm in this paper is not randomly selected.

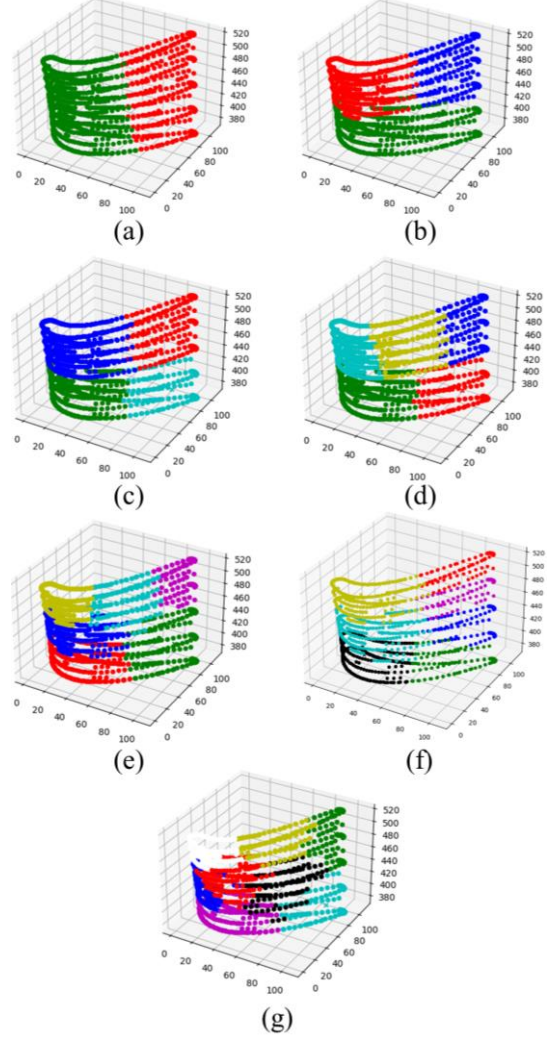


**Fig. 8** K-means clustering results of the blade(the value of  $k$  in (a)~(g) is 2~8 in order, units in the figures: mm)

It can be seen from Figure 9 and Figure 10 that when the clustering value  $k=2$  and the fixed number of points is 2, the experimental results at this time are optimal, that is, the accuracy and efficiency of segmentation are both optimal. The reasons are as follows: First, the total number of nodes divided by the improved octree partition method is reduced by 711 compared with the total number of nodes partitioned by the traditional octree partition method. This means that the

improved octree segmentation method eliminates the invalid space, thereby improving the accuracy of the segmentation. At this time, the improved octree segmentation method improves the accuracy of the segmentation by 12.80% compared with the traditional octree segmentation method; The second is that the split time of the improved octree segmentation method at this time is reduced by 4.82s compared with the segmentation time of the traditional octree

segmentation method. This means that the improved octree partition method can quickly divide the space, thereby increasing the efficiency of the partition. At this time, the improved octree partition method has a 40.88% increase in the efficiency of the partition compared with the traditional octree partition method. The above results can prove the effectiveness of the improved octree segmentation method proposed in this paper.

**Table 1** Comparison of the total number of split nodes between the traditional octree partition method and the improved octree partition method (Here, FNOP means fixed number of points, and TNON means total number of nodes)

FNOP/piece \ TNON/piece		1	2	3	4	5	6	7	8	9	10
Traditional algorithm		11809	5553	3209	2425	2017	1633	1313	1137	985	881
Improved algorithm by introducing <i>k-means</i> clustering method	<i>k</i> =2	11718	4842	3154	2402	1954	1506	1298	1130	1026	970
	<i>k</i> =3	12131	5315	3371	2451	1995	1555	1283	1131	963	899
	<i>k</i> =4	12052	5324	3444	2340	1820	1500	1308	1092	948	828
	<i>k</i> =5	11933	5205	3317	2317	1853	1549	1317	1101	989	813
	<i>k</i> =6	12238	5326	3486	2382	1846	1534	1358	1166	1006	862
	<i>k</i> =7	12151	5407	3479	2351	1879	1575	1255	1111	1015	829
	<i>k</i> =8	12304	5256	3440	2286	1904	1568	1264	1064	896	832

**Table 2** Comparison of the split time between the traditional octree segmentation method and the improved octree segmentation method (Here, FNOP means fixed number of points, and ST means split time)

FNOP/piece \ ST/s		1	2	3	4	5	6	7	8	9	10
Traditional algorithm		17.11	11.79	4.55	3.48	3.06	2.47	2.02	1.88	1.64	1.50
Improved algorithm by introducing <i>k-means</i> clustering method	<i>k</i> =2	17.07	6.97	4.65	4.13	3.29	2.56	2.37	1.87	1.76	1.68
	<i>k</i> =3	14.35	6.95	4.50	3.75	2.83	2.28	1.84	1.70	1.53	1.57
	<i>k</i> =4	20.15	10.02	6.37	4.34	3.50	3.08	2.75	2.33	2.06	1.93
	<i>k</i> =5	25.42	11.25	7.28	5.06	4.42	3.63	3.17	2.79	2.57	2.03
	<i>k</i> =6	16.70	8.69	5.65	4.26	3.29	2.94	2.68	2.37	2.09	1.95
	<i>k</i> =7	16.17	8.53	5.41	4.17	3.30	2.89	2.58	2.31	2.18	1.98
	<i>k</i> =8	19.37	9.43	7.11	5.35	4.47	3.86	3.32	2.89	2.59	2.44

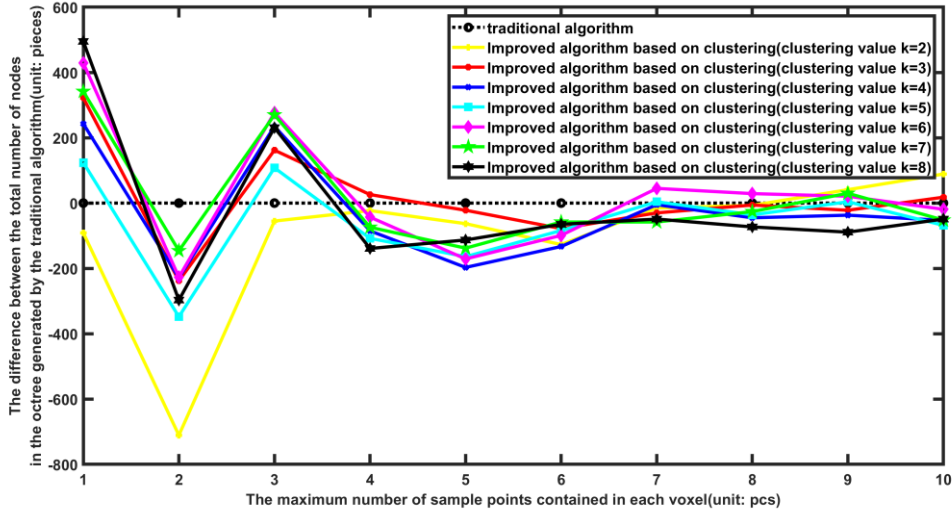


**Fig. 9** Comparison of the total number of split nodes between the traditional octree partition method and the improved octree partition method

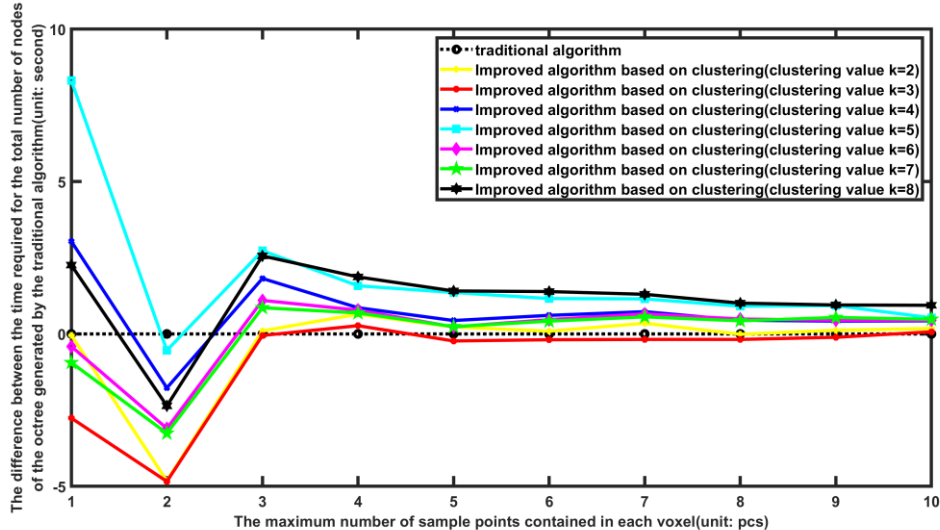


**Fig. 10** Comparison of the split time between the traditional octree segmentation method and the improved octree segmentation method

#### 4.2 Collision detection experiment results and analysis

This paper verifies the proposed collision detection algorithm from two aspects: one is to verify the algorithm by developing a matching blade collision detection software, and the other is to perform experimental verification through processing experiments.

In terms of algorithm verification, this paper develops a set of abrasive belt grinding and polishing the Blisk collision detection software

based on the above theoretical methods. The collision detection process is shown in Figure 11(a). In terms of experimental verification, this paper has realized the experimental verification of the collision detection of the Blisk abrasive belt grinding and polishing processing by a robot, and the collision detection process diagram is shown in Figure 11(b). The experimental results obtained from algorithm verification and experimental verification are shown in Table 3 and Table 4, respectively, the visualization results are shown in

Figure 12(a) and Figure 12(b) respectively.

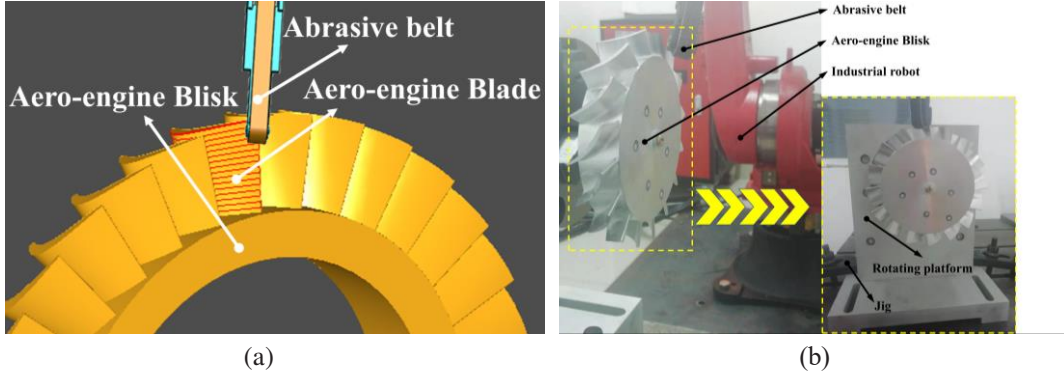


**Fig. 11** The algorithm verification of the collision detection of the Blisk of the belt grinding (a), and the experimental verification based on the robot processing (b)

**Table 3** Algorithm verification results for collision detection of the Blisk with belt grinding

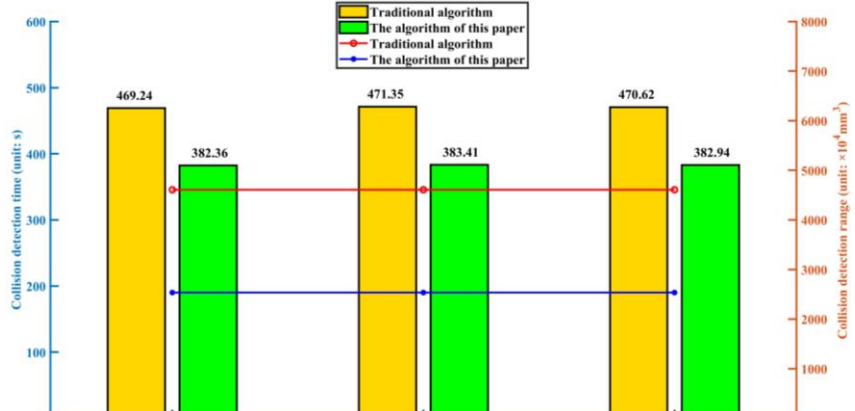
Attributes \ methods		Traditional algorithm	The algorithm of this paper	Optimization percentage
Collision detection range (unit: $\times 10^4 \text{mm}^3$ )	1	4608.00	2534.40	45%
	2	4608.00	2534.40	45%
	3	4608.00	2534.40	45%
	Average	4608.00	2534.40	45%
Collision detection time (unit: s)	1	469.24	382.36	18.52%
	2	471.35	383.41	18.66%
	3	470.62	382.94	18.63%
	Average	470.40	382.90	18.60%

Due to the introduction of clustering algorithm in the algorithm in this paper, the Blisk and the point cloud of the blade are divided into multiple parts from a whole, and each part is divided into different clusters. As a result, the collision space required by the re-divided point cloud area is more compact, which improves the accuracy of collision detection. From Table 3 and Table 4, it can be concluded that the accuracy of the collision detection of the algorithm in this paper is about 45% higher than that of the traditional algorithm

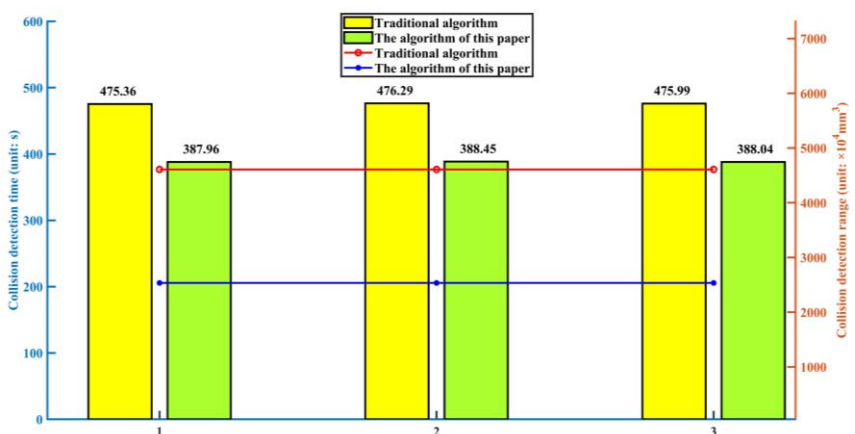
on average. In terms of collision detection time, because the algorithm in this paper can eliminate the space that does not participate in collision detection, this greatly reduces the number of nodes divided by the octree, thereby reducing the traversal time required for collision detection. It can also be concluded from Table 3 and Table 4 that the collision detection efficiency of the algorithm in this paper is 18.60% and 18.44% higher than the traditional algorithm respectively.

**Table 4** Validation results of robotic machining experiments for the collision detection of the Blisk of belt grinding

Attributes \ methods		Traditional algorithm	The algorithm of this paper	Optimization percentage
Collision detection range (unit: $\times 10^4 \text{mm}^3$ )	1	4608.00	2534.40	45%
	2	4608.00	2534.40	45%
	3	4608.00	2534.40	45%
Average	Average	4608.00	2534.40	45%
Collision detection time (unit: s)	1	475.36	387.96	18.39%
	2	476.29	388.45	18.44%
	3	475.99	388.04	18.48%
Average	Average	475.88	388.15	18.44%



(a)



(b)

**Fig. 12** The visualization result of algorithm verification (a) and the visualization result of experimental verification (b)

Finally, this paper obtains the comparative

analysis results of the coordinate measuring

machine (CMM) measurement data of the cross-sectional profile of a certain Blade of the Blisk before and after the abrasive belt grinding process, as shown in Figure 13, Table 5 and Figure 14.

From the results of the comparative analysis of the error data before and after processing, the average error of the blade area A is reduced from 0.0238mm to 0.0183mm, the average error of the B area is reduced from 0.0234mm to 0.0154mm, the average error of the C area is reduced from

0.0251mm to 0.0181mm, and the average error of the D area is reduced from 0.0228mm to 0.0168mm, which meets the actual relevant technical requirements.

Therefore, in the actual machining test, the method proposed in this paper not only effectively realizes the collision detection of the abrasive belt grinding of the Blisk, but also guarantees the accuracy of the abrasive belt grinding of the Blisk.

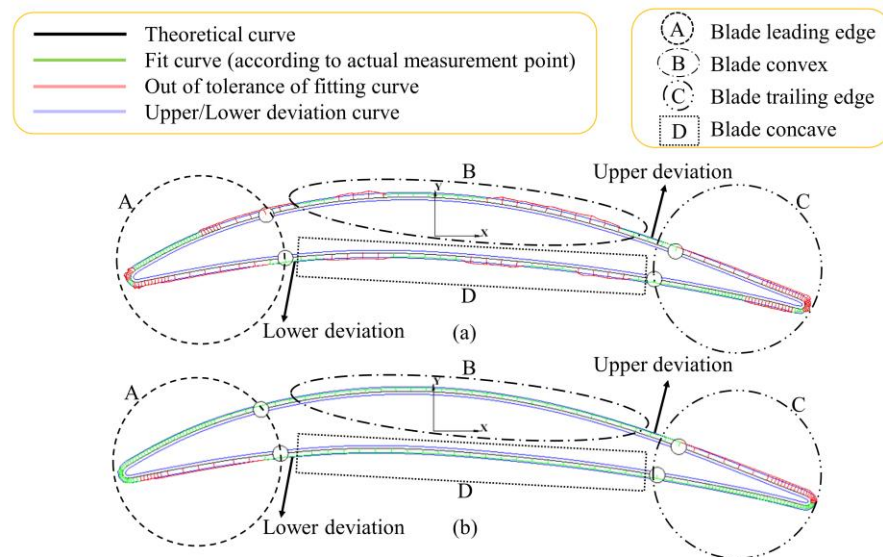


**Fig. 13** CMM measurement profile comparison of the Blade before(a) and after(b) processing

**Table 5** The error of each area of the Blade before and after processing

	Detection area	minError/mm	maxError/mm	averError/mm	stdError/mm
Before processing	A	0.0197	0.0282	0.0238	0.0028
	B	0.0188	0.0271	0.0234	0.0024
	C	0.0200	0.0290	0.0251	0.0023
	D	0.0191	0.0260	0.0228	0.0021
After processing	A	0.0137	0.0235	0.0183	0.0031
	B	0.0116	0.0199	0.0154	0.0025
	C	0.0134	0.0223	0.0181	0.0029
	D	0.0133	0.0197	0.0168	0.0021

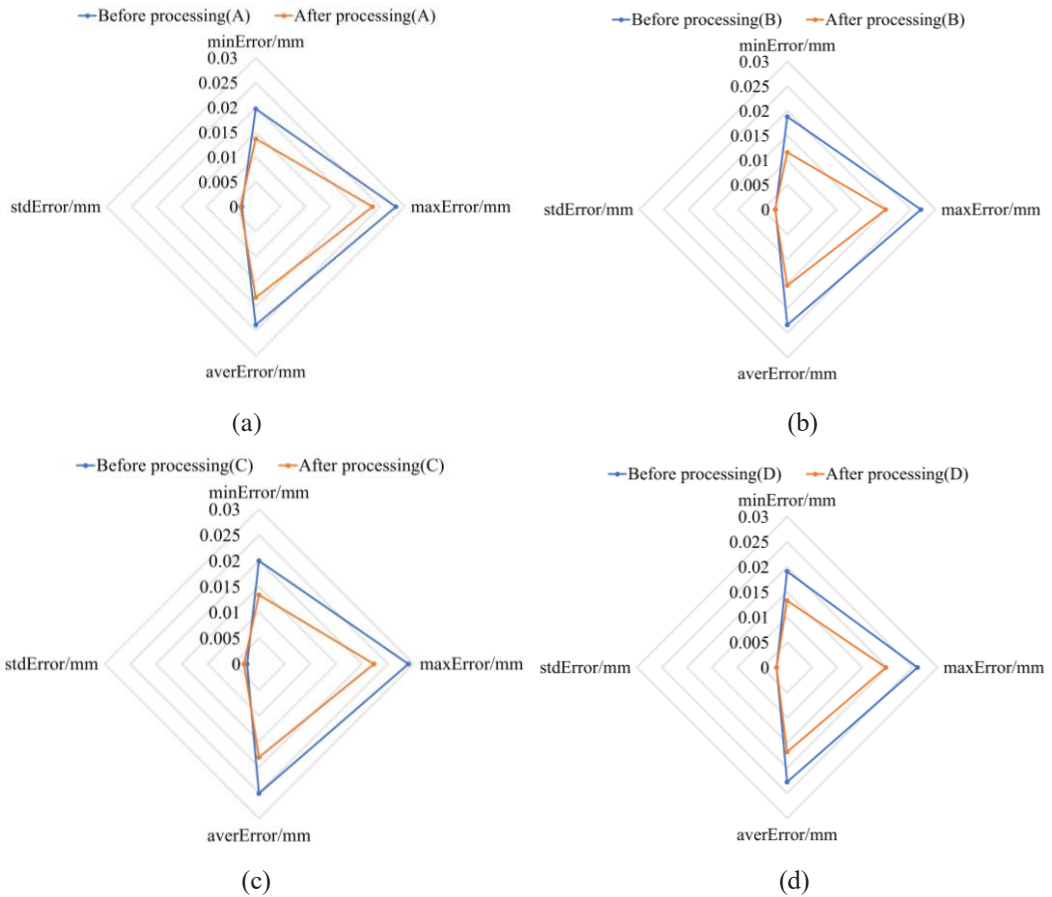


**Fig. 14** Error comparison of each area of the Blade before and after processing((a) area A, (b) area B, (c) area C, and (d) area D)

## 5 Conclusion

In this paper, an improved octree segmentation method based on *k-means* clustering algorithm is proposed, and then based on the improved octree segmentation method, a collision detection algorithm for abrasive belt grinding of the Blisk is given. Finally proved the feasibility of the algorithm proposed in this paper through software verification and experimental verification. The main conclusions of this paper are as follows:

- (1) By introducing the *k-means* clustering algorithm, the traditional octree segmentation method is improved, and the improved octree segmentation method can better eliminate the redundant space. The experimental results obtained on a single blade show that the improved algorithm improves the accuracy of segmentation by 12.80% and the efficiency of segmentation

by 40.88% compared with the traditional algorithm.

- (2) The feasibility of the collision detection algorithm proposed in this paper is verified through algorithm verification and experimental verification. The experimental results of the algorithm verification show that the accuracy of the collision detection of the algorithm in this paper is 45% higher than the traditional algorithm, and the efficiency of the collision detection is 18.60% higher than the traditional algorithm; the experimental results show that the accuracy of the collision detection algorithm in this paper is 45% higher than the traditional algorithm, and the efficiency of collision detection is 18.44% higher than the traditional algorithm.

However, this paper only realizes the collision

detection research in the ordinary Blisk grinding, and it has not been able to cover the more complex Blisk samples such as the closed Blisk. In future research, on the one hand, the collision detection algorithm will continue to be optimized, and on the other hand, more research on collision detection and avoidance of more complex surfaces will be considered.

## Funding

The Fundamental Research Funded by Sichuan Science and Technology Plan (grant number: 2020YFG0407/2020JDRC0173).

## References

1. Huang Z, Wei PX, Li C, Wang HY, Wang JY (2020) Aero-engine blade profile reconstruction based on adaptive step size bat algorithm and visualization of machining error. Proceedings of the Institution of Mechanical Engineers, Part C: Journal of Mechanical Engineering Science 234: 49-65
2. Zou L, Huang Y, Zhang GJ, Cui XP (2019) Feasibility study of a flexible grinding method for precision machining of the TiAl-based alloy. Materials and Manufacturing Processes 34: 1160-1168
3. Xuan W, Cai YL (2017) The tool path planning of composed surface of big-twisted blisk. Procedia Engineering 174: 392-401
4. Shigematsu T, Koike R, Kakinuma Y, Aoyama T, Ohnishi K (2016) Sensorless tool collision detection for multi-axis machine tools by integration of disturbance information. Procedia CIRP 57: 658-663
5. Xu XH, Zhu DH, Zhang HY, Yan SJ, Ding H (2019) Application of novel force control strategies to enhance robotic abrasive belt grinding quality of aero-engine blades. Chinese Journal of Aeronautics 32: 2368-2382
6. Ilies, HT (2009) Continuous collision and interference detection for 3D geometric models. Journal of Computing and Information Science in Engineering 9: 1-7
7. Zhang T, Su JW (2018) Collision-free planning algorithm of motion path for the robot belt grinding system. International Journal of Advanced Robotic Systems 15: 1-13
8. Ren X, Kuhlenkötter B, Müller H (2006) Simulation and verification of belt grinding with industrial robots. International Journal of Machine Tools and Manufacture 46: 708-716
9. Tang YH, Hou J, Wu TT (2018) Hybrid collision detection algorithm based on particle conversion and bounding box. Journal of Harbin Engineering University 39: 1695-1701
10. Raj Prasanth D, Shunmugam MS (2020) Geometry-based Bend Feasibility Matrix for bend sequence planning of sheet metal parts. International Journal of Computer Integrated Manufacturing 33: 515-530
11. Zou YN, Liu PX, Yang CS, Li CQ, Cheng QQ (2017) Collision detection for virtual environment using particle swarm optimization with adaptive cauchy mutation. Cluster Comput 20: 1765–1774
12. Sang Z, Wang TY, Zou XX, Xu HN (2016) Research on Online Collision Detection Algorithm of CNC Machine Tools. KEM 693: 1780-1785
13. Tang TD, Bohez ELJ (2015) A new collision avoidance strategy and its integration with collision detection for five-axis NC machining. The International Journal of Advanced Manufacturing Technology 81: 1247-1258
14. Huang Y, Xiao GJ, Zou L (2019) Current situation and development trend of robot precise belt grinding for aero-engine blade. ACTA AERONAUTICAET ASTRONAUTICA SINICA 40(3): 1-20
15. Lin XB, Lin FN (2016) Hybrid hierarchical collision detection based on data reuse.

Telkomnika (Telecommunication Computing Electronics and Control) 14(3): 1077-1082

16. Abbas SA, Aslam A, Rehman AU, Abbasi WA, Arif S, Kazmi SZH (2020) K-Means and K-Medoids: Cluster Analysis on Birth Data Collected in City Muzaffarabad, Kashmir. IEEE Access, pp. 151847-151855
17. Abdelrahman TS (2020) Cooperative Software-hardware Acceleration of K-means on a Tightly Coupled CPU-FPGA System. ACM Transactions on Architecture and Code Optimization 17: 1-24
18. Tang M, Manocha D, Yoon SE et al (2011) VolCCD: Fast continuous collision culling between deforming volume meshes. ACM Transactions on Graphics 30: 1-15
19. El-Sousy FFM (2016) Intelligent mixed H<sub>2</sub>/H<sub>∞</sub> adaptive tracking control system design using self-organizing recurrent fuzzy-wavelet-neural-network for uncertain two-axis motion control system. Applied Soft Computing 41: 22-50
20. Huang Z, Wei PX, Wan CB, Wang HY, Wu XG, Wang JY (2020) Collision detection method of blisk grinding and polishing. Jisuanji Jicheng Zhizao Xitong/Computer Integrated Manufacturing Systems, CIMS 26: 3350-3358

## Figures

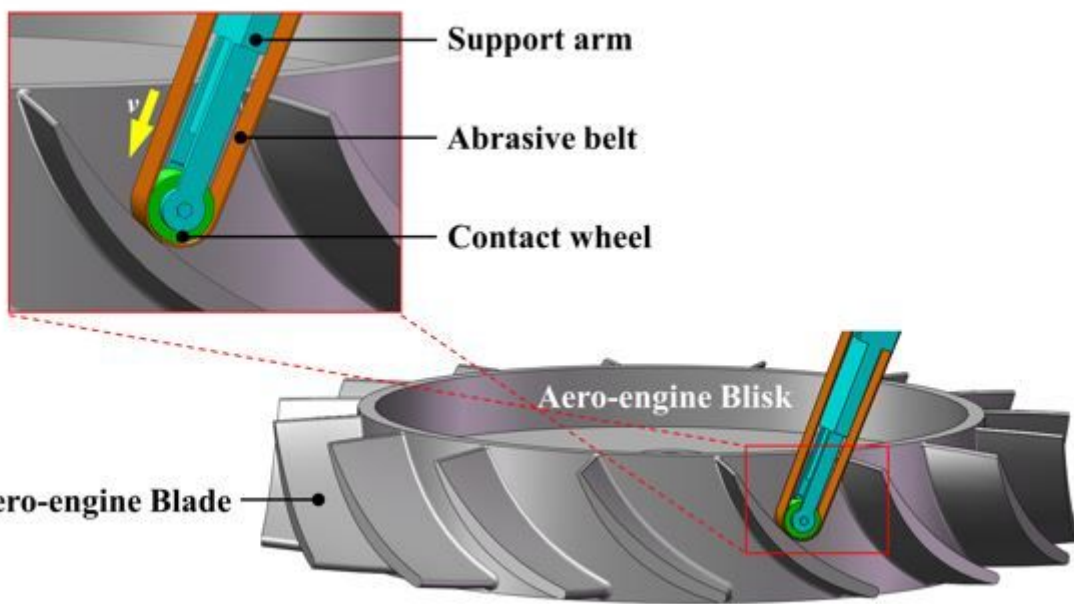


Figure 1

The principle diagram of belt grinding the Blisk

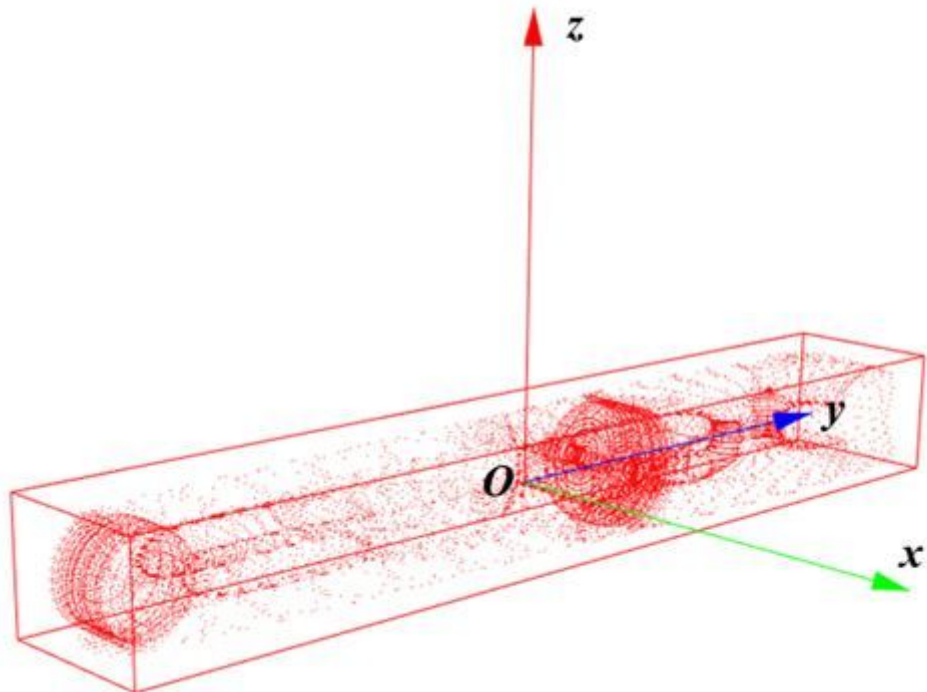
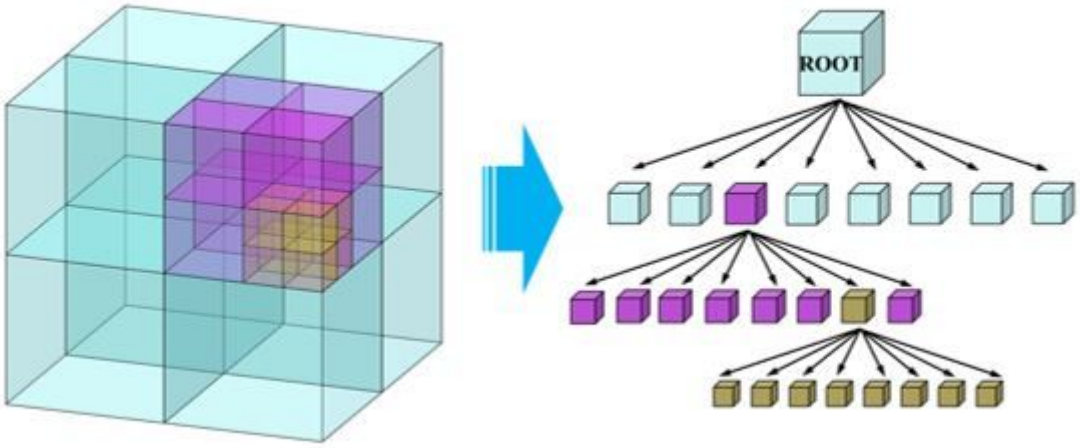


Figure 2

OBB bounding box model of the abrasive belt



**Figure 3**

Schematic diagram of octree segmentation method

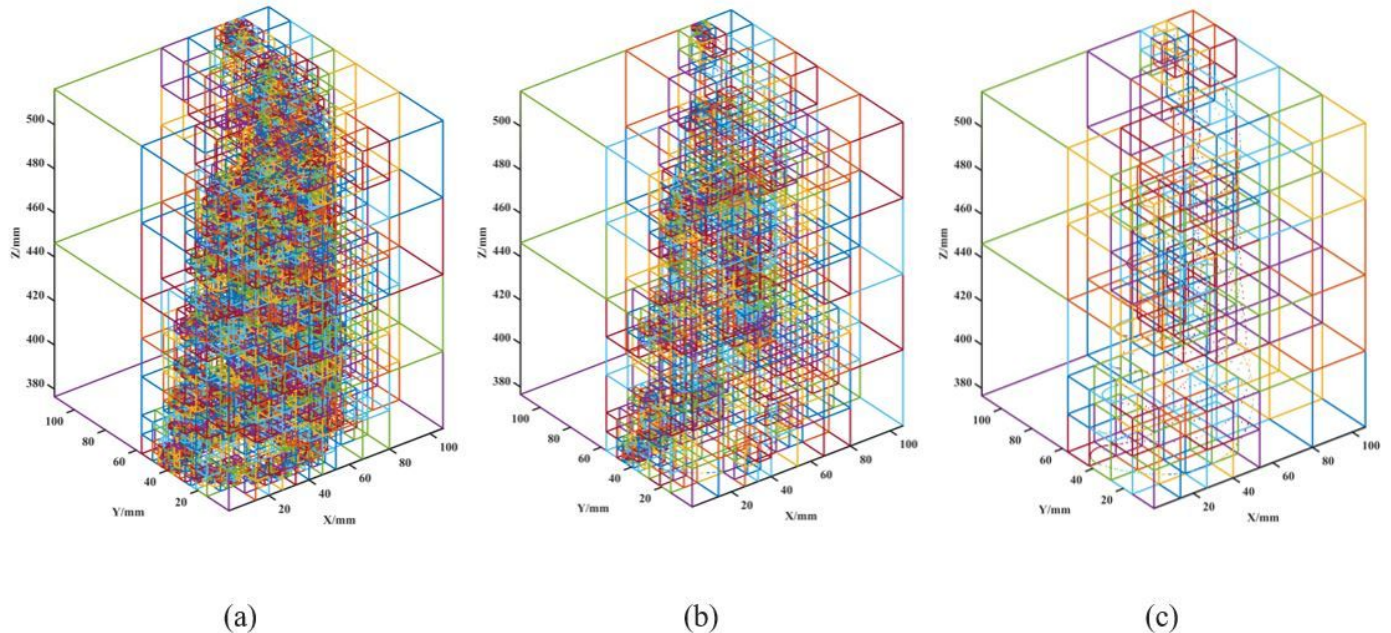


**Figure 4**

Octree segmentation results of the blade under different fixed points((a) the number of fixed points is 2, (b) the number of fixed points is 10, (c) the number of fixed points is 50)

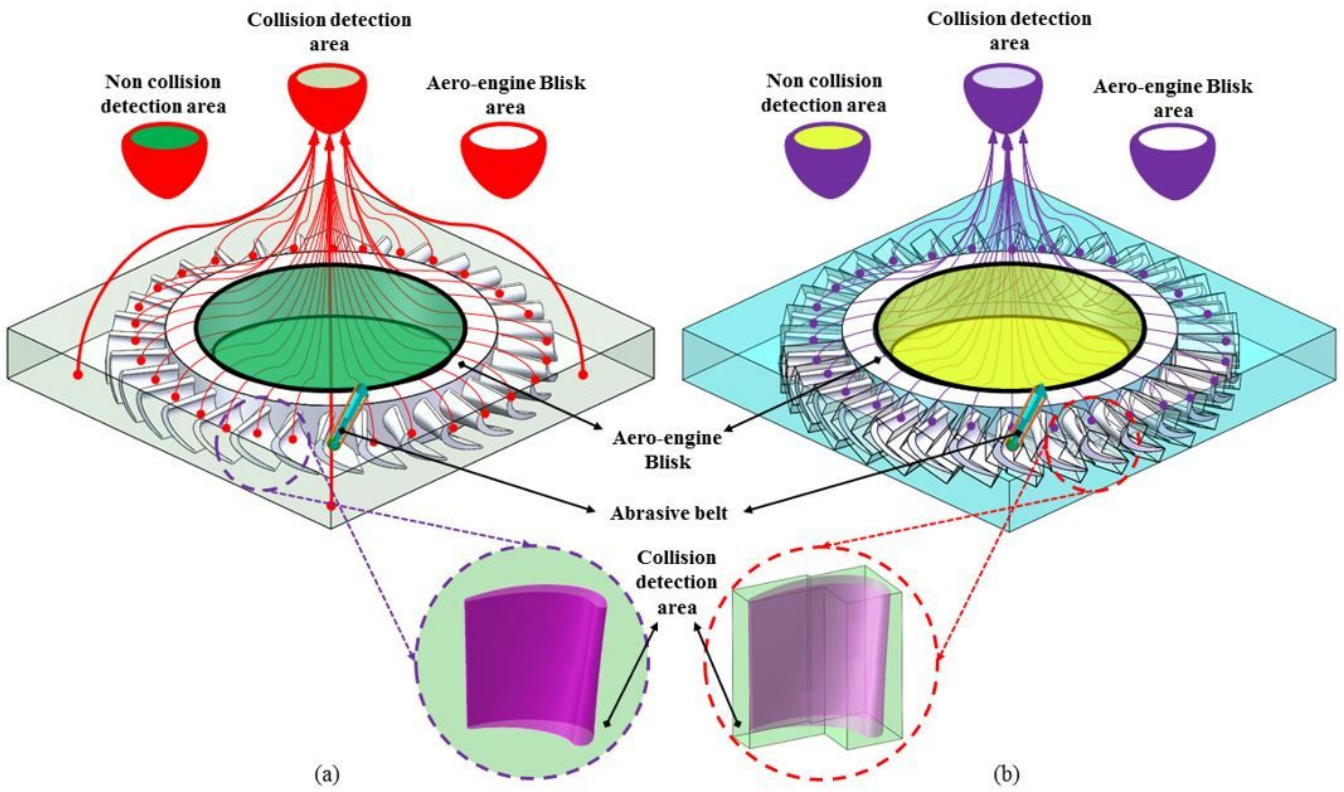


**Figure 5**

Comparison of spatial segmentation between traditional octree segmentation method and improved octree segmentation method ((a) traditional octree segmentation method, (b) improved octree segmentation method)

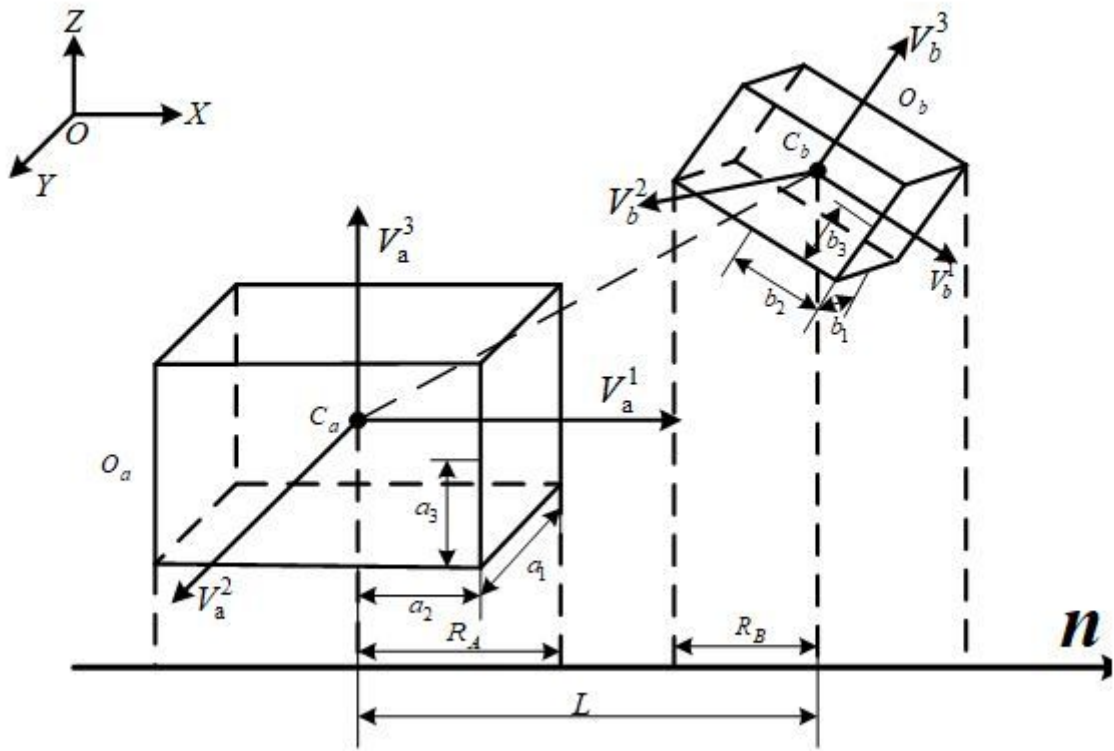


**Figure 6**

The principle diagram of the collision detection of the separation axis method [20]

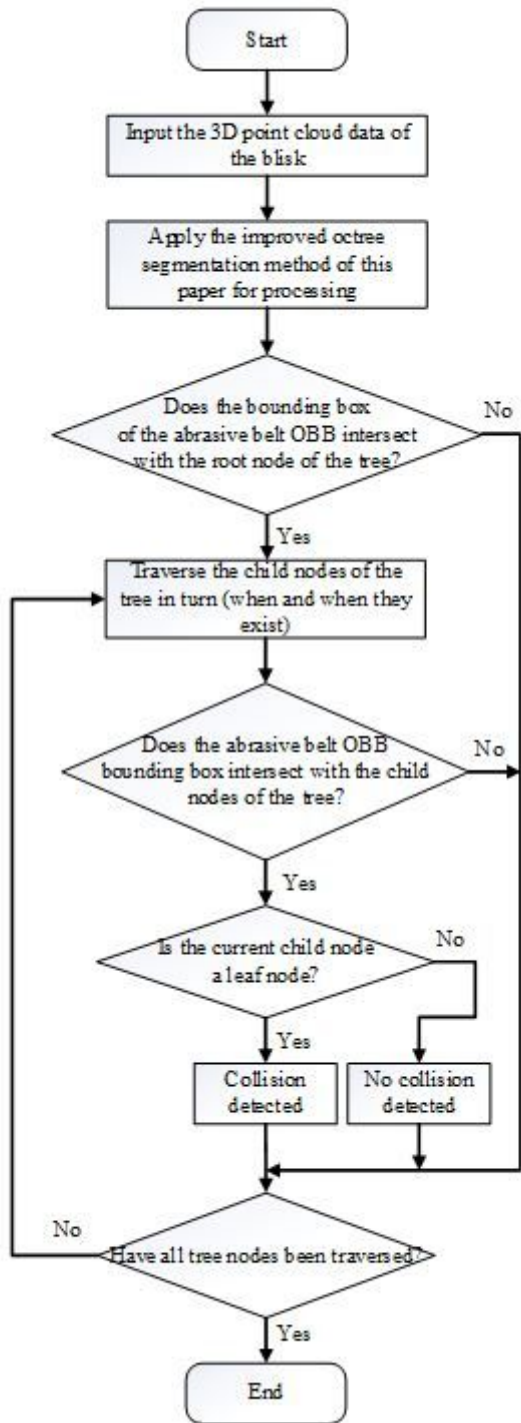


**Figure 7**

Flow chart of collision detection algorithm in this paper

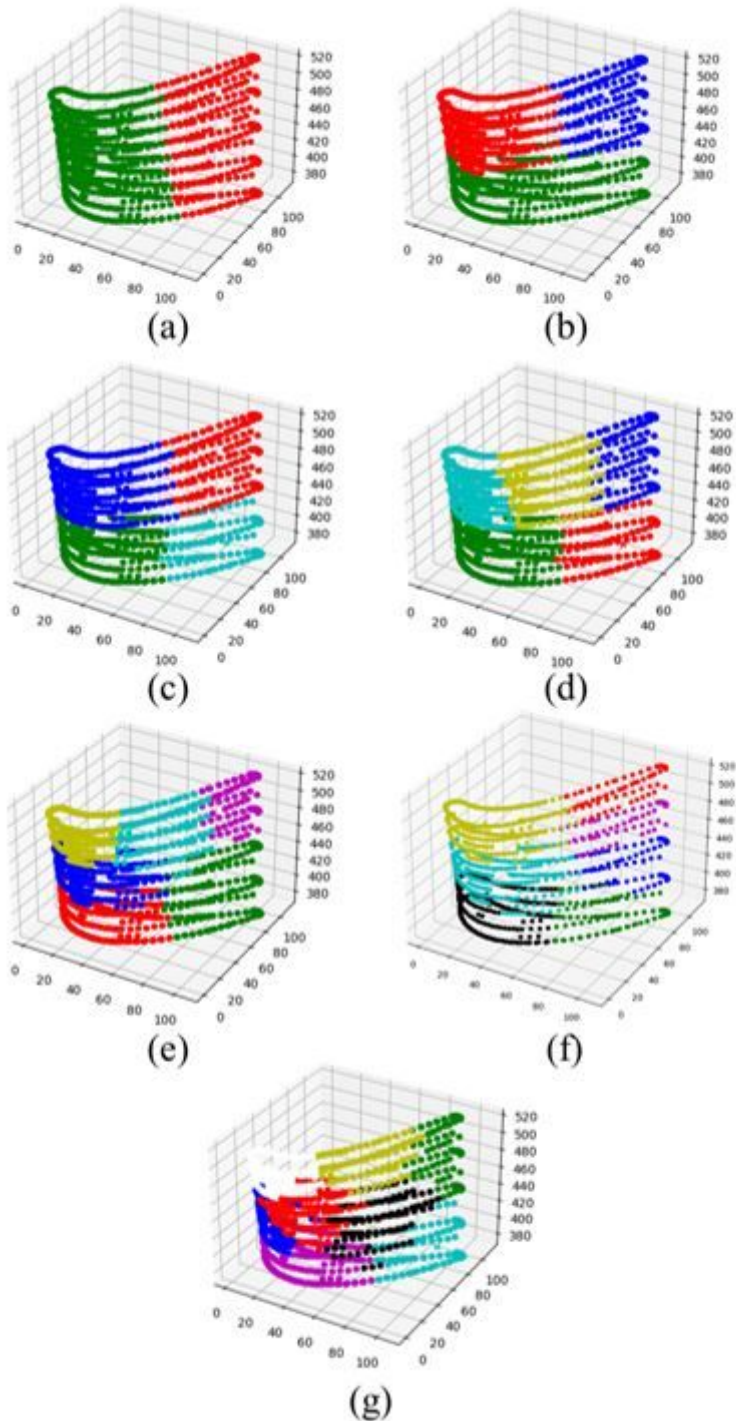


**Figure 8**

K-means clustering results of the blade (the value of k in (a)–(g) is 2–8 in order, units in the figures: mm)

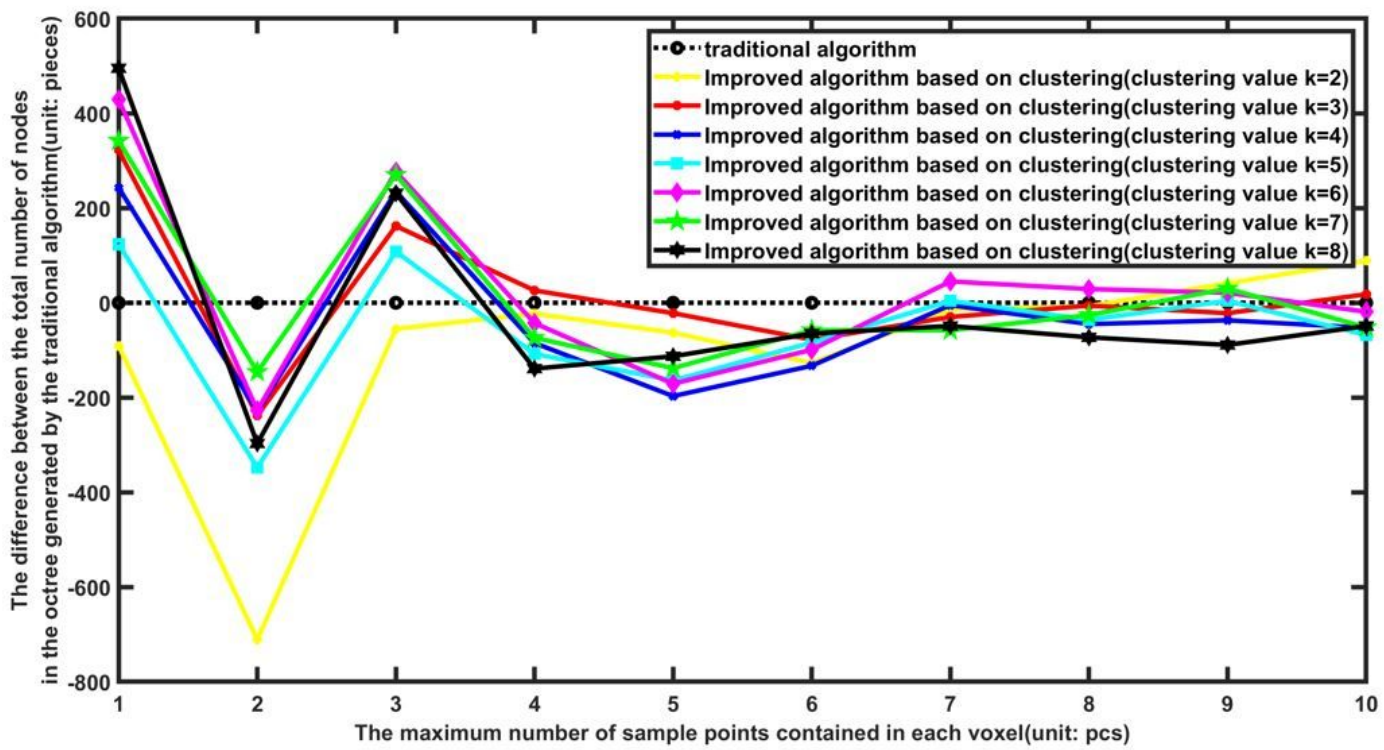
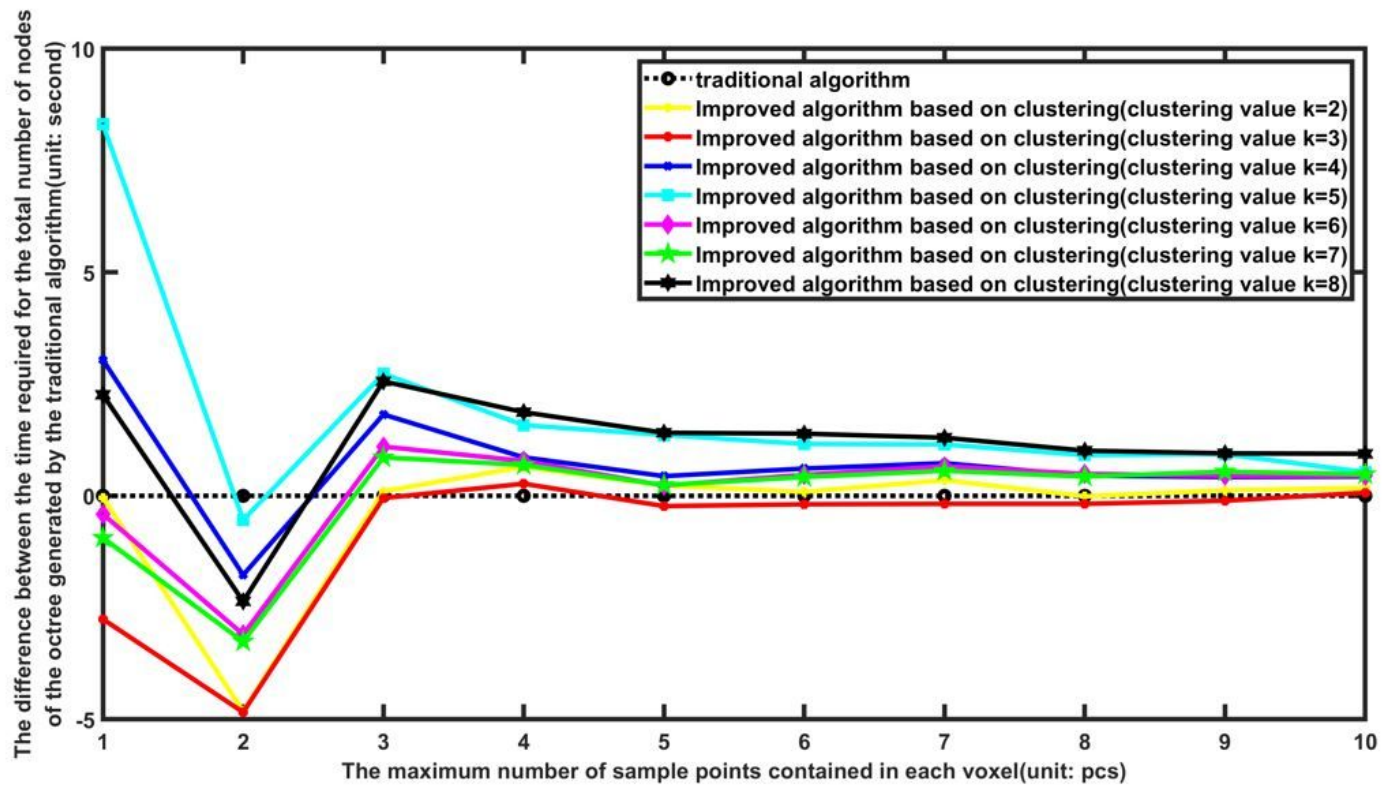


Figure 9

Comparison of the total number of split nodes between the traditional octree partition method and the improved octree partition method



**Figure 10**

Comparison of the split time between the traditional octree segmentation method and the improved octree segmentation method

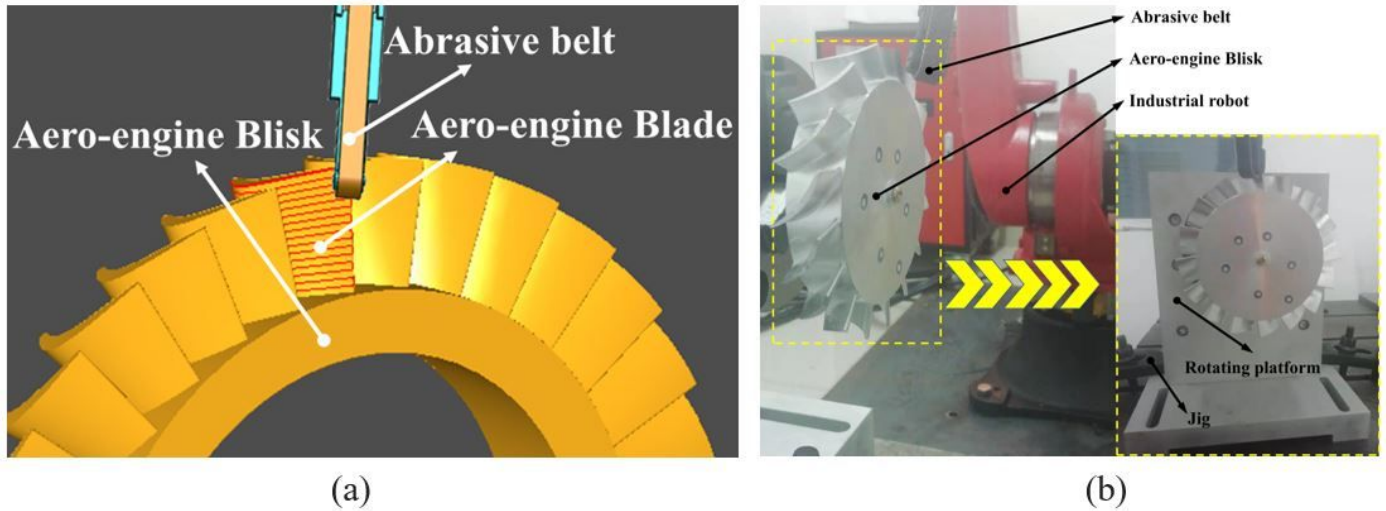
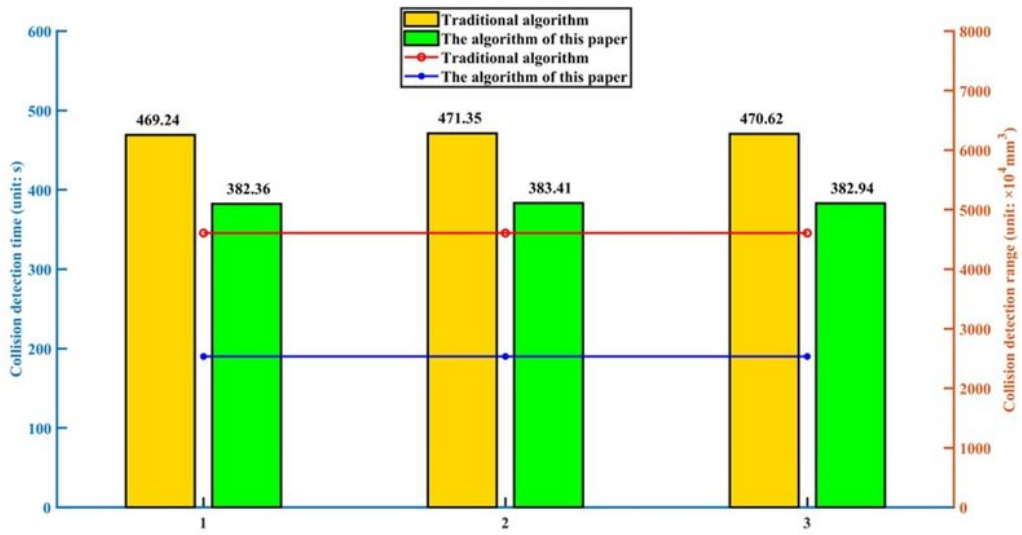
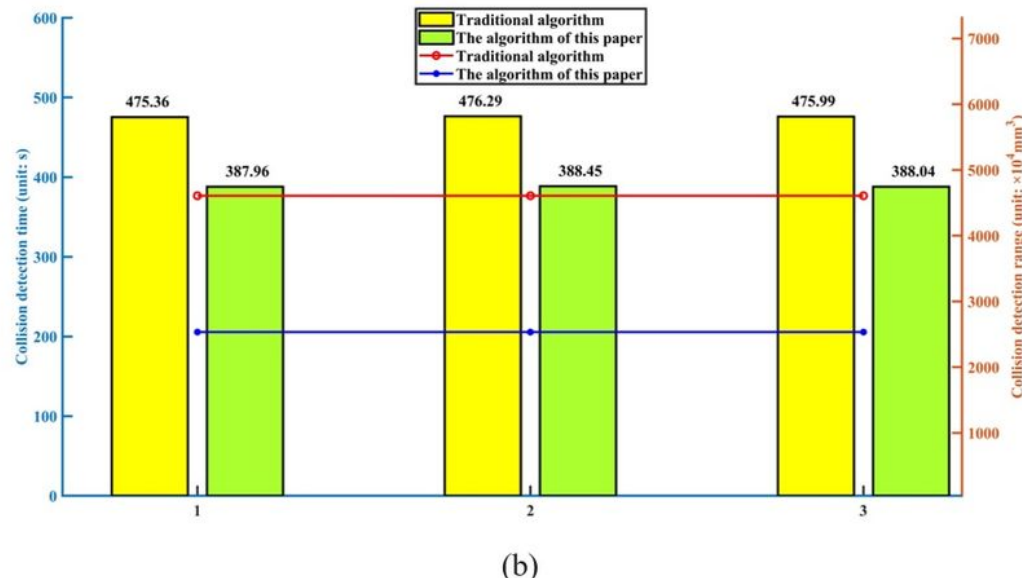


**Figure 11**

The algorithm verification of the collision detection of the Blisk of the belt grinding (a), and the experimental verification based on the robot processing (b)



(a)



(b)

**Figure 12**

The visualization result of algorithm verification (a) and the visualization result of experimental verification (b)

— Theoretical curve  
 — Fit curve (according to actual measurement point)  
 - Out of tolerance of fitting curve  
 - Upper/Lower deviation curve

(A) Blade leading edge  
 (B) Blade convex  
 (C) Blade trailing edge  
 (D) Blade concave

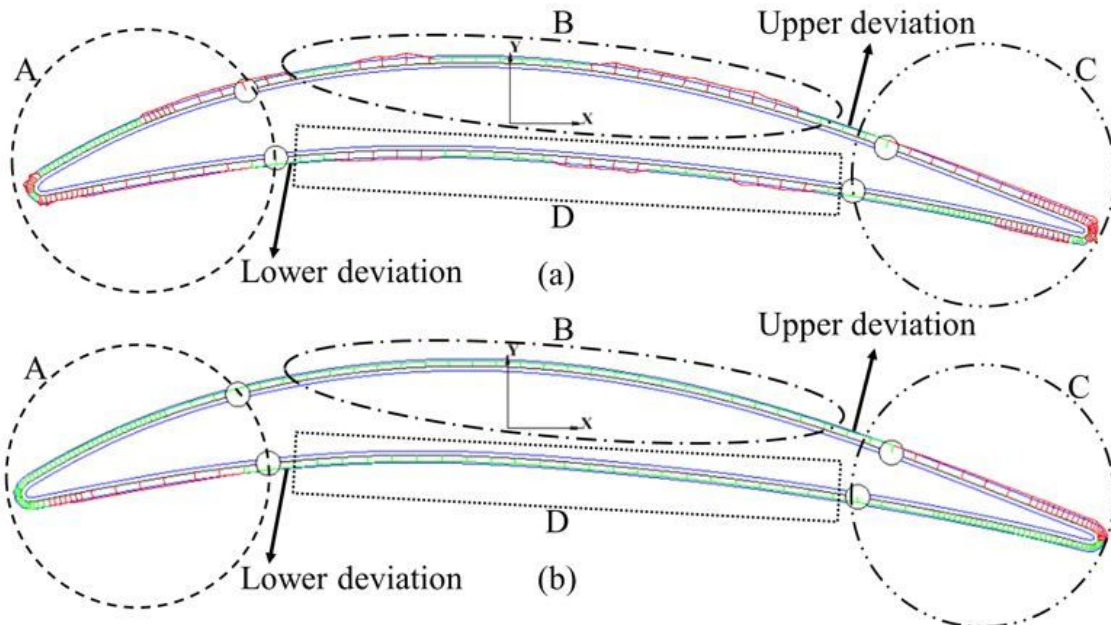


**Figure 13**

CMM measurement profile comparison of the Blade before(a) and after(b) processing

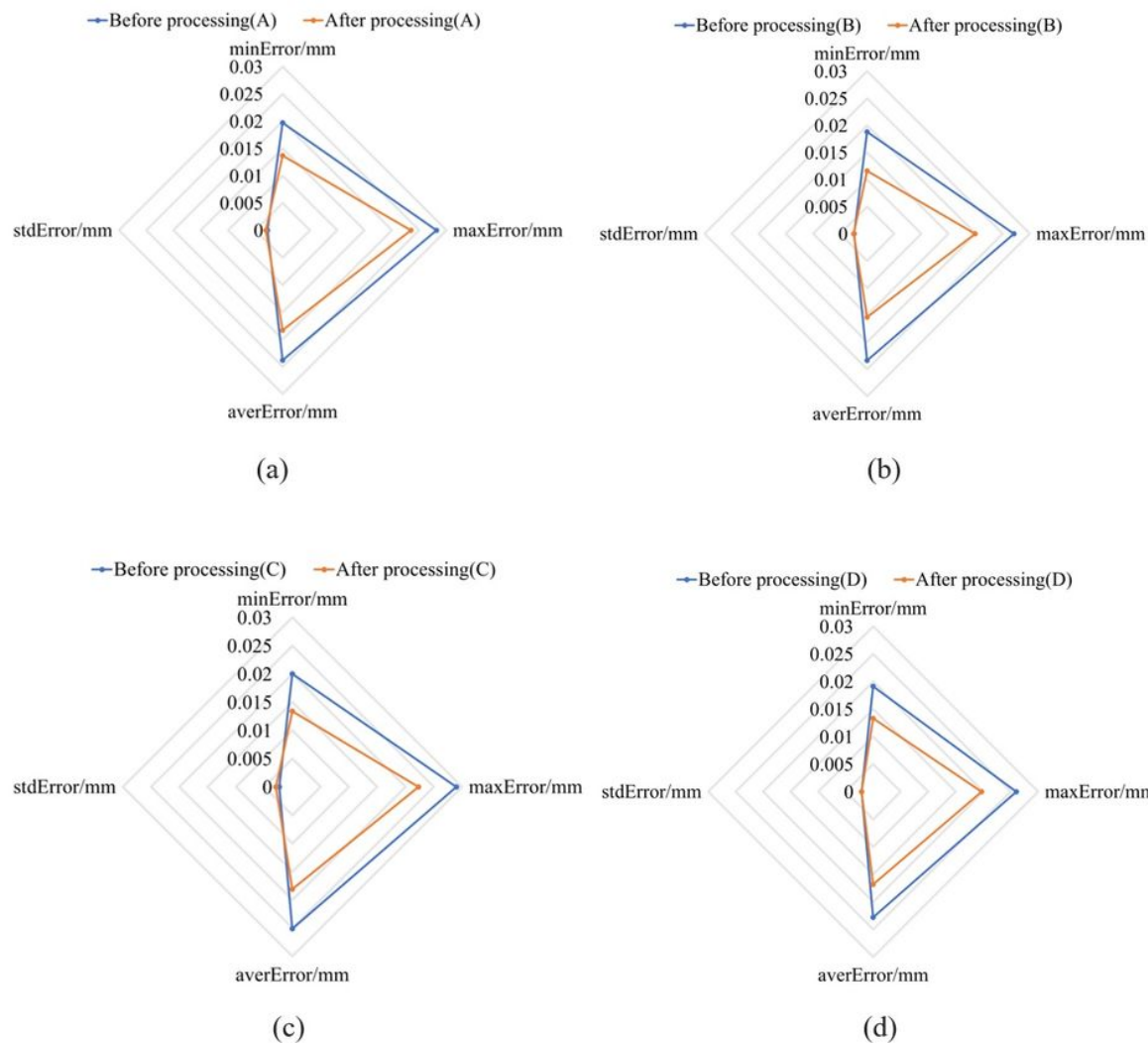


**Figure 14**

Error comparison of each area of the Blade before and after processing((a) area A, (b) area B, (c) area C, and (d) area D)